

# Assessment of exposure to X-rays during patient positioning at the proton eye radiotherapy facility at IFJ PAN, Kraków

Dominika Adamczyk,  
Barbara Dulny,  
Tomasz Horwacik,  
Jan Swakoń,  
Paweł Olko

**Abstract.** At the Institute of Nuclear Physics of the Polish Academy of Sciences (IFJ PAN, Kraków, Poland) the proton eye radiotherapy facility has recently been developed and is now fully operational. A set of two X-ray RAD-14 Varian medical systems tubes are used to obtain orthogonal images of the patient's eyeball undergoing radiotherapy with tantalum clips already attached to its surface to delineate the tumour volume. We assessed the dose received by the patient from multiple X-ray exposures during the patient positioning procedure. Measurements of  $K_{\text{air}}$  were performed using various types of ionization chambers and MCP-N thermoluminescent (TL) detectors and calculated using the PCXMC code. Good agreement between measurements and calculations was found. The mean absorbed dose to the brain was measured using TL detectors placed inside the head of a Rando anthropomorphic phantom used in simulation of the patient positioning procedure. The measured maximum incident air kerma absorbed during the entire procedure of patient positioning was found not to exceed 7 mGy, while the mean absorbed dose to the brain did not exceed 2 mSv.

**Key words:** eye proton therapy • exposure assessment • patient positioning

## Introduction

Proton therapy is an advanced radiotherapy (RT) technique currently in use at a limited number of centres around the world. The unique properties of the proton beam allow the treatment volume to be precisely irradiated while sparing the surrounding normal tissues and critical volumes behind the eyeball.

High precision of patient positioning is required in proton eye radiotherapy. Prior to patient positioning, a set of tantalum clips is surgically attached to the eyeball to delineate the tumour volume. Next, individual immobilizing elements (i.e. an individual mask, and a bite-block) are prepared, the patient is placed in the therapy chair, and finally, a series of orthogonal X-ray images is taken to precisely establish the eyeball location for radiotherapy planning purposes. From digital X-ray images taken at different eye positions the X-ray images of the clips are compared with their apparent locations within the eclipse treatment planning system (TPS) which is then used to create a full three-dimensional (3-D) representation of the patient's eye, of the intra-ocular tumour and of the planned dose distribution from the proton beam.

D. Adamczyk, B. Dulny, T. Horwacik, J. Swakoń✉,  
P. Olko

The Henryk Niewodniczański Institute of Nuclear Physics, Polish Academy of Sciences (IFJ PAN),  
152 Radzikowskiego Str., 31-342 Kraków, Poland,  
Tel.: +48 12 662 8087, Fax: +48 12 662 8458,  
E-mail: Jan.Swakon@ifj.edu.pl

Received: 2 June 2011

Accepted: 28 September 2011

The aim of this study was to assess the absorbed dose received by the patient from multiple X-ray exposures during the patient positioning procedure at the proton eye radiotherapy facility at the IFJ PAN, Kraków.

### Patient positioning system

The patient positioning system at IFJ PAN consists of a computer-controlled patient treatment chair (Schär Engineering Ltd.), an eye positioning system including the eye fixation light-diode, individually prepared elements to immobilize the patient's head and a pair of RAD-14 Varian medical systems X-ray tubes with beam axes set at 90° to each other. The position of the treatment chair can be varied along three orthogonal axes and rotated around the vertical axis, all to within a few hundredths of a millimetre. This setup, combined with individually manufactured immobilizing elements, allows for accurate and repetitive patient positioning during the whole irradiation procedure consisting of several fractions.

An important part of the patient positioning procedure and also of the following verification of treatment setup are a set of two simultaneously obtained orthogonal X-ray images of the eye with the marker clips in place, enabling tumour borders to be identified. All X-ray images are stored on phosphor plates and read out digitally by a Kodak CR 260 point-of-care are reader. Using custom made code – ImageComparator (T. Kajdrowicz), the actual position of the tantalum clips obtained from X-ray images is compared with the position of DICOM RT images, imported from the accepted plan from the TPS. Entering to the ImageComparator the actual position of the chair and performing series of translations and rotations of the RT images, the program calculates a new position of the treatment chair in which a new set of X-ray images is performed.

### Dose measurements in X-ray exposures

For X-ray examinations, radiation exposure is usually defined as the surface dose in air at the position where the beam axis enters the patient's body or the surface of the phantom [1, 14, 15]. X-ray exposure dosimetry aims at estimating the mean dose delivered to the patient, for a given X-ray equipment setup and diagnostic procedure. In diagnostic radiology effective dose and skin dose are considered. Because in this case it is not possible to directly and non-invasively measure the dose contributed by the radiation to individual organs, organ doses have to be evaluated from measurements of incident or entrance surface air kerma [2, 14, 15].

Parallel-plate ionization chambers are the main instruments for measuring dose in the diagnostic X-ray energy range, but other dosimeters, such as thermoluminescent detectors (TLDs) are also widely used, mainly for dose measurements inside physical phantoms or for patient skin dose measurements [2, 4, 13, 15]. Other methods for determining organ and tissue doses are Monte Carlo (MC) simulations or analytical calculations using computer codes, such as PCXMC or PREPARE [4, 13, 15, 16].

### Materials and methods

Measurements of air kerma,  $K_{\text{air}}$ , were carried out over three locations: at two points nearest to the lateral and axial X-ray tubes, corresponding to the left temple and the occiput, and at the isocentre of the proton beam. The selection of the first two points was based on the definition of X-ray exposure. Measurements in the last position were carried out because the isocentre is the reference point in radiotherapy planning, corresponding to the centre of the tumour during all therapeutic sessions. Doses were measured using various types of ionization detectors: a PTW Freiburg type TM32002 1000 cm<sup>3</sup> ionization chamber [8], a PTW Freiburg type 31013 0.3 cm<sup>3</sup> ionization chamber [9], a PTW Freiburg type 32005 30 cm<sup>3</sup> ionization chamber [10], a RTI Electronics AB Barracuda multimeter with a R100 dose detector [11] and using LiF:Mg,Cu,P (MCP-N) thermoluminescent detectors (TLDs). The centres of all detector active volumes were first positioned at the isocentre. Detectors were then moved closer to the axial or lateral X-ray tube by varying the position of the treatment chair.

All measurements by ionization chambers were corrected for ambient air pressure and temperature. The calibration factors for each ionization chamber and electrometer were obtained from the Laboratory for Calibration Radiation Protection Instruments (NLW) at IFJ PAN except for the Barracuda multimeter which was calibrated at RTI Electronics AB in Sweden. Measurements obtained by TLDs were energy-corrected as the X-ray energy spectrum to which they were exposed differed from the energy spectrum at which they were calibrated (Cs-137). To establish proper energy correction factors, X-ray energy spectra for both X-ray tubes were estimated using the SpekCalc code [7]. The LiF:Mg,Cu,P TLD correction factors were calculated from their measured energy response [5] and the calculated photon energy spectra. Before each irradiation all TL detectors were annealed for 10 min at 240°C and for 5 min at 100°C before their readout, using a RA'94 portable reader-analyser TLD system.

The Rando anthropomorphic male phantom of 175 cm height and 73.5 kg weight was used for measurements of the absorbed dose to the head. The phantom has no arms or legs. It consists of a natural human skeleton cast inside a tissue-like material. The phantom is divided into 2.5 cm slices, each containing a 3 × 3 cm grid of holes for inserting TL detectors. Dose measurements were performed using MCP-N pellets placed in selected holes. Time consuming TLD measurements were performed only for the optimized X-ray filtration setup.

### Setup parameters and geometry of exposure

According to the current Polish regulations, X-ray images for medical diagnostics of the head should be performed using the voltage of 70 to 85 kV from a distance of 100 to 150 cm [1]. In the proton eye radiotherapy facility in Kraków these criteria cannot be fulfilled, as the source-to-image (SID) and object-to-image (OID) are fixed at 2285 and 560 mm for the lateral X-ray

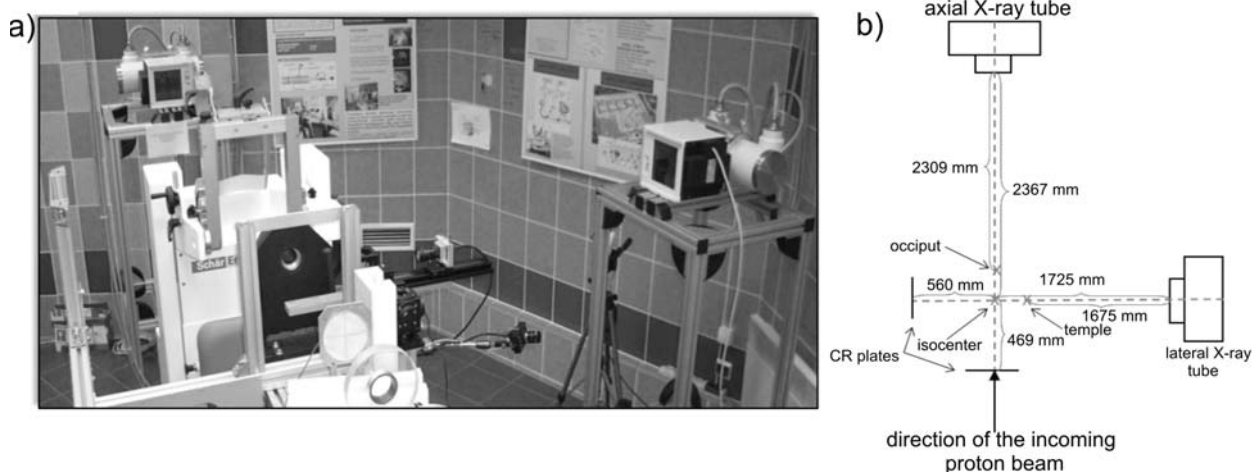


**Fig. 1.** The set of two X-ray tubes used for orthogonal X-ray imaging to determine the position of the tumour in the eyeball for ocular proton radiotherapy: a – down-beam view of the X-ray tubes in the treatment room; b – configuration used for measurements in this work.

tube, and at 2836 and 469 mm for the axial X-ray tube, respectively (Fig. 1). These large SID and OID values affect the quality of X-ray images, especially for the axial X-ray tube. However, high quality X-ray images are not required in proton therapy because images are only used in the TPS for estimating the position of the tumour with respect to the coordinates of the proton beam. For this reason, we consider the exposure parameters of the X-ray tubes to be satisfactory, if the positions of the markers and of the positioning crosses are clearly distinguishable in the X-ray images, even while image contrast and signal to noise ratio are relatively poor.

Prior to setting the basic X-ray tube parameters at 85 kV, 40 mAs and 75 kV, 8 mAs for the axial and lateral X-ray tubes respectively, several images of the Rando Alderson's head with tantalum clips attached to its right eye were taken. The above working parameters for the lateral and axial X-ray tubes were selected, based on the quality of the obtained X-ray images (Fig. 2).

Measurements of  $K_{air}$  were carried out using different tube voltages (ranging between 70 and 100 kV) and different current-time products (ranging between 5 and 50 mAs). Measurements were performed with and without additional filtration of 1 mm Al and 0.1 mm Cu. The inherent filtration of both X-ray tubes with collimators is equal to 2.7 mm Al. Measurements of dose inside the Rando phantom were performed using the basic radiation parameters of 85 kV and 40 mAs for the axial X-ray tube and 75 kV and 8 mAs for the lateral X-ray tube. The radiation field was set to  $5 \times 5$  collimator scale units, giving radiation field sizes at the isocentre of  $10.5 \times 10.5$  cm and  $14.8 \times 14.8$  cm for the lateral and the axial X-ray tubes, respectively. These radiation field sizes are considered to be the largest applicable field sizes during the patient positioning procedure. The proper field sizes are selected individually, depending on the patient's anatomical features and tumour size, and in most cases are much smaller. Measurements

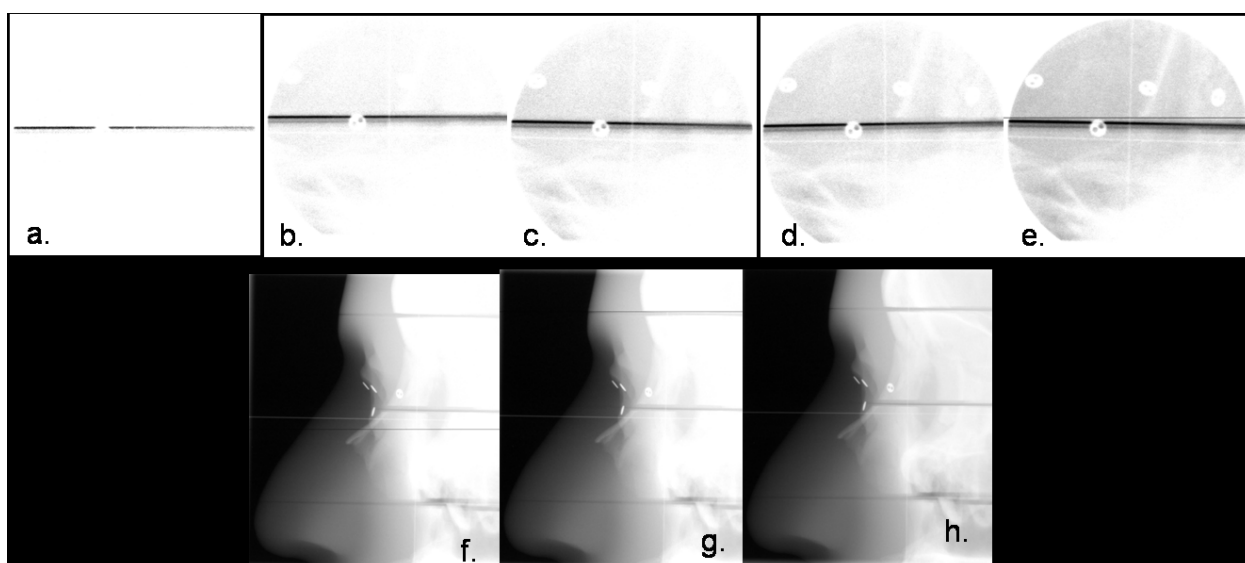


**Fig. 2.** X-ray images obtained at different tube voltages and current-time products in the determination of optimum working parameters for the axial X-ray tube: a – 66 kV, 32 mAs; b – 80 kV, 32 mAs; c – 82 kV, 32 mAs; d – 85 kV, 32 mAs; e – 85 kV, 40 mAs and for the lateral X-ray tube: f – 66 kV, 10 mAs; g – 70 kV, 5 mAs; h – 75 kV, 10 mAs. Small round objects visible on the X-ray images are tantalum clips attached to the right eye and temple of the Rando phantom. The light vertical and horizontal lines are positioning hairlines which aid in determining the position of the isocentre in proton beam coordinates.

**Table 1.** Mean values of the measured  $K_{\text{air}}$  (mGy) per single exposure from the axial X-ray tube

| Detector                       | Mean $K_{\text{air}}$ (mGy) |   |                          |   |
|--------------------------------|-----------------------------|---|--------------------------|---|
|                                | Isocentre                   |   | Occiput                  |   |
|                                | No additional filtration    | With additional filters<br>1 mm Al, 0.1 mm Cu | No additional filtration | With additional filters<br>1 mm Al, 0.1 mm Cu |
| TM32002 1000 cm <sup>3</sup>   | 0.374                       | 0.164   | 0.315                    | 0.171   |
| 32005 30 cm <sup>3</sup>       | 0.426                       | 0.201   | 0.455                    | 0.218   |
| 31013 0.3 cm <sup>3</sup>      | 0.401                       | 0.192   | 0.423                    | 0.202   |
| Barracuda (R100 dose detector) | 0.409                       | 0.189   | 0.411                    | 0.193   |
| MCP TLD                        | –                           | 0.203   | –                        | 0.215   |

**Table 2.** Mean values of the measured  $K_{\text{air}}$  (mGy) per single exposure from the lateral X-ray tube

| Detector                       | Mean $K_{\text{air}}$ (mGy) |   |                          |   |
|--------------------------------|-----------------------------|---|--------------------------|---|
|                                | Isocentre                   |   | Left temple              |   |
|                                | No additional filtration    | With additional filters<br>1 mm Al, 0.1 mm Cu | No additional filtration | With additional filters<br>1 mm Al, 0.1 mm Cu |
| TM32002 1000 cm <sup>3</sup>   | 0.111                       | 0.050   | 0.115                    | 0.053   |
| 32005 30 cm <sup>3</sup>       | 0.128                       | 0.057   | 0.140                    | 0.061   |
| 31013 0.3 cm <sup>3</sup>      | 0.124                       | 0.054   | 0.135                    | 0.059   |
| Barracuda (R100 dose detector) | 0.126                       | 0.058   | 0.141                    | 0.061   |
| MCP TLD                        | –                           | 0.064   | –                        | 0.068   |

performed with the 1000 cm<sup>3</sup> ionization chamber were exceptional. Due to the large dimensions of this ionization chamber, the largest applicable X-ray field size did not cover its entire detection volume. Having verified that the response of this chamber was fairly constant over a wide range of field sizes, for measurements using the 1000 cm<sup>3</sup> ionization chamber, 7 × 7 and 8 × 8 collimators scale units were set for the axial and the lateral X-ray tubes, respectively.

### Monte Carlo calculations

The patients' organ doses and effective dose following medical X-ray examinations were calculated using the PCXMC 2.0 code. In calculations of effective dose this code uses the new (ICRP-103, 2007) and the old (ICRP-60, 1991) tissue weighting factors. Mean values of absorbed doses to the organ are averaged over the organ volume. The anatomical data used in PCXMC are from the mathematical hermaphrodite phantom models of Cristy and Eckerman [6]. Monte Carlo calculations are based on stochastic mathematical simulation of interactions between photons and matter. Three types of interaction are considered: photoelectric absorption, Rayleigh and Compton scattering. Photons are generated from an isotropic point source into the solid angle specified by the focal distance and the X-ray field size. The geometry and patient data can be selected [3, 6, 12].

In this study the phantom of an adult of standard height and mass was used for the MC simulation. The exposure geometry used during  $K_{\text{air}}$  measurements (Fig. 1b) was defined. The coordinates of the reference point ( $x_{\text{Ref}}$ ,  $y_{\text{Ref}}$ ,  $z_{\text{Ref}}$ ) inside the phantom through which the central axis of the X-ray beam is directed, was set to (0, 0, 89) for the axial X-ray tube and to (5, -4, 88.5) for the lateral X-ray tube. For dose calculations, the

basic radiation parameters were used for each X-ray tube. For calculations of the mean dose absorbed to the brain, the results of measurements of  $K_{\text{air}}$  using PTW Freiburg type 31013 0.3 cm<sup>3</sup> ionization chamber were used as input dose quantity. The incident air kerma was calculated with and without additional filtration of 1 mm Al and 0.1 mm Cu. The anode angle for both tubes was set to 12°.

### Results and discussion

Results pertaining to a given X-ray tube are given per single X-ray exposure while those pertaining to dose absorbed in the brain – per single simultaneous exposure from both X-ray tubes or per patient setup procedure involving 5 simultaneous exposures, as indicated. In Tables 1 and 2 we present the values of mean  $K_{\text{air}}$  measured with different types of ionization chambers for the axial and the lateral X-ray tubes set at the basic radiation parameters of 85 kV, 40 mAs and 75 kV, 8 mAs, respectively. In Table 3, the results of PCXMC calculations of entrance air kerma using the relevant parameters, i.e. X-ray tube voltage, tube current-time product, total filtration and focal spot to skin dis-

**Table 3.** Values of  $K_{\text{air}}$  per single exposure, as evaluated by PCXMC software. Calculations of  $K_{\text{air}}$  for each X-ray tube were carried out at the location where the beam axis crosses the phantom body

|   | Entrance $K_{\text{air}}$ (mGy) |
|---|---------------------------------|
| Axial X-ray tube                              | 0.417                           |
| Axial X-ray tube with additional filtration   | 0.185                           |
| Lateral X-ray tube                            | 0.130                           |
| Lateral X-ray tube with additional filtration | 0.052                           |

**Table 4.** Relative differences between the results of measurements and those of calculations for the axial and the lateral X-ray tubes

| Detector                       | Difference = $100 \times (K_{\text{air, calculations}} - K_{\text{air, measurements}}) / K_{\text{air, calculations}}$ (%) |                    |   |                    |
|--------------------------------|--|--------------------|---|--------------------|
|                                | Axial X-ray tube   | Lateral X-ray tube | Axial X-ray tube                                | Lateral X-ray tube |
|                                | without additional filters   |                    | with additional filtration (1 mm Al, 0.1 mm Cu) |                    |
| TM32002 1000 cm <sup>3</sup>   | 24.4   | 11.7               | 7.7   | -2.1               |
| 32005 30 cm <sup>3</sup>       | -9.2   | -7.5               | -17.6   | -17.5              |
| 31013 0.3 cm <sup>3</sup>      | -1.5   | -3.7               | -9.0  | -13.7              |
| Barracuda (R100 dose detector) | 1.3  | -8.3               | -4.2  | -17.5              |
| MCP TLD                        | -  | -                  | -16.0   | -31.0              |

**Table 5.** Uncertainties ( $1\sigma$ ) of  $K_{\text{air}}$  measurements for all methods used in this study (see text)

|                                | One SD* (%) |
|--------------------------------|-------------|
| TM32002 1000 cm <sup>3</sup>   | < $\pm 4$   |
| 32005 30 cm <sup>3</sup>       | < $\pm 5$   |
| 31013 0.3 cm <sup>3</sup>      | < $\pm 2$   |
| Barracuda (R100 dose detector) | $\pm 5$     |
| MCP TLD                        | < $\pm 1.5$ |
| PCXMC calculations             | $\pm 16$    |

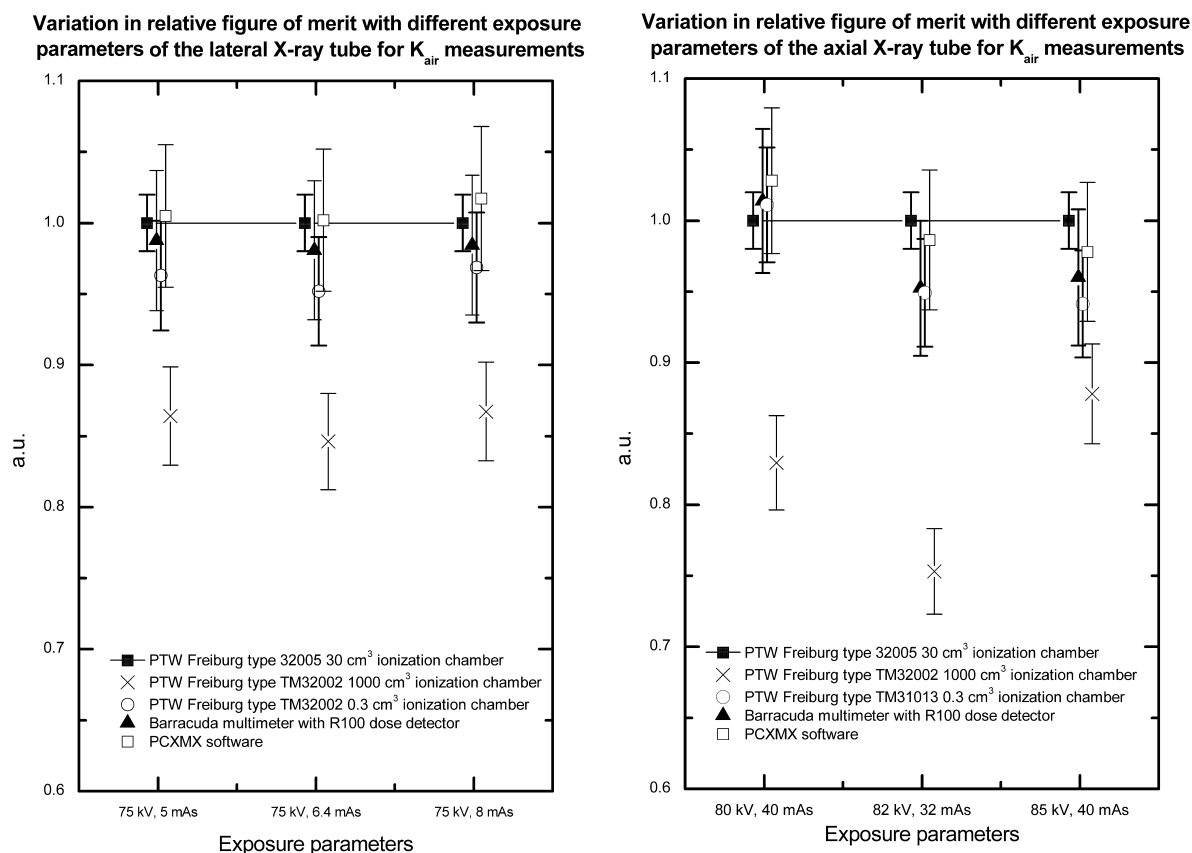
\*SD – standard deviation.

tance, are shown for the axial and lateral X-ray tubes. In Table 4, we compare the results of measurements and of MC calculations of  $K_{\text{air}}$ . In Table 5, we list the relative uncertainties ( $1\sigma$ ) of dose evaluations for all methods used, as based on the distribution of repeated results of each measurement (5 repetitions per measurement point), or on the distribution of readouts of TLDs

(5 detectors per measurement point). The uncertainty of the PCXMC calculations is taken from the software documentation.

It may be seen from the above results that the air kerma,  $K_{\text{air}}$ , from one simultaneous exposure with both X-ray tubes does not exceed 550  $\mu\text{Gy}$ . Additional aluminium and copper filters (1 mm Al, 0.1 mm Cu) reduce this value to 250  $\mu\text{Gy}$ . Since a patient positioning session typically involves 4 to 5 synchronous X-ray exposures, the total air kerma would not exceed 3 mGy, the reference dose level for lateral skull radiography. It follows that the value of air kerma from X-ray exposures integrated over the whole positioning procedure will not exceed 15 mGy, or 7 mGy if filtration is added.

Changes in the relative figure of merit (FOM) with different exposure parameters and types of ionization detectors (Fig. 3) show that the agreement between the measured and calculated values of  $K_{\text{air}}$  in our study

**Fig. 3.** Variation of the relative figure of merit with the choice of different exposure parameters for the axial or lateral X-ray tubes, obtained with the use of different ionization detectors. For plotting, variation of the relative figure of merit data from  $K_{\text{air}}$  measurements at the isocentre without additional filtration was used. Error bars correspond to one standard deviation (SD) of 5 repetitive measurements.

**Table 6.** Average absorbed dose in the brain obtained from TL measurements in the Rando phantom from one set of X-ray images taken simultaneously

| Slice no. | $D_i$ (mGy) |
|-----------|-------------|
| 1         | 0.027       |
| 2         | 0.069       |
| 3         | 0.109       |
| 4         | 0.095       |
| 5         | 0.065       |

is within 1.5% for the lateral and within 2.5% for the axial X-ray tube. Only the 1000 cm<sup>3</sup> ionization chamber significantly underestimated the measured  $K_{\text{air}}$ . The primarily goal of using the 1000 cm<sup>3</sup> chamber was its high sensitivity. However, the results of the present work clearly show that the large ionization chamber is not suitable for measurements of small X-ray fields

in proton eye radiotherapy, because in the used geometry the large chamber volume is not uniformly irradiated.

Table 6 contains the results of measurements of the mean absorbed dose in slices of the Rando phantom which are relevant for evaluating the total brain dose. Since the absorbed dose to the brain from one simultaneous exposure is quite low, especially if additional filtration is used, five sequential exposures of the Rando phantom were performed in order to improve the measurement accuracy. We found the measured mean dose to the brain from one simultaneous exposure to be equal to 0.0825 mGy, which compares quite well with the results of PCXMC simulations (0.0807 mGy). Two-dimensional (2-D) distributions of the absorbed dose in slices of the relevant parts of the head of the Rando phantom, obtained using the Surfer (Golden Software) plotting tool, are shown in Fig. 4.

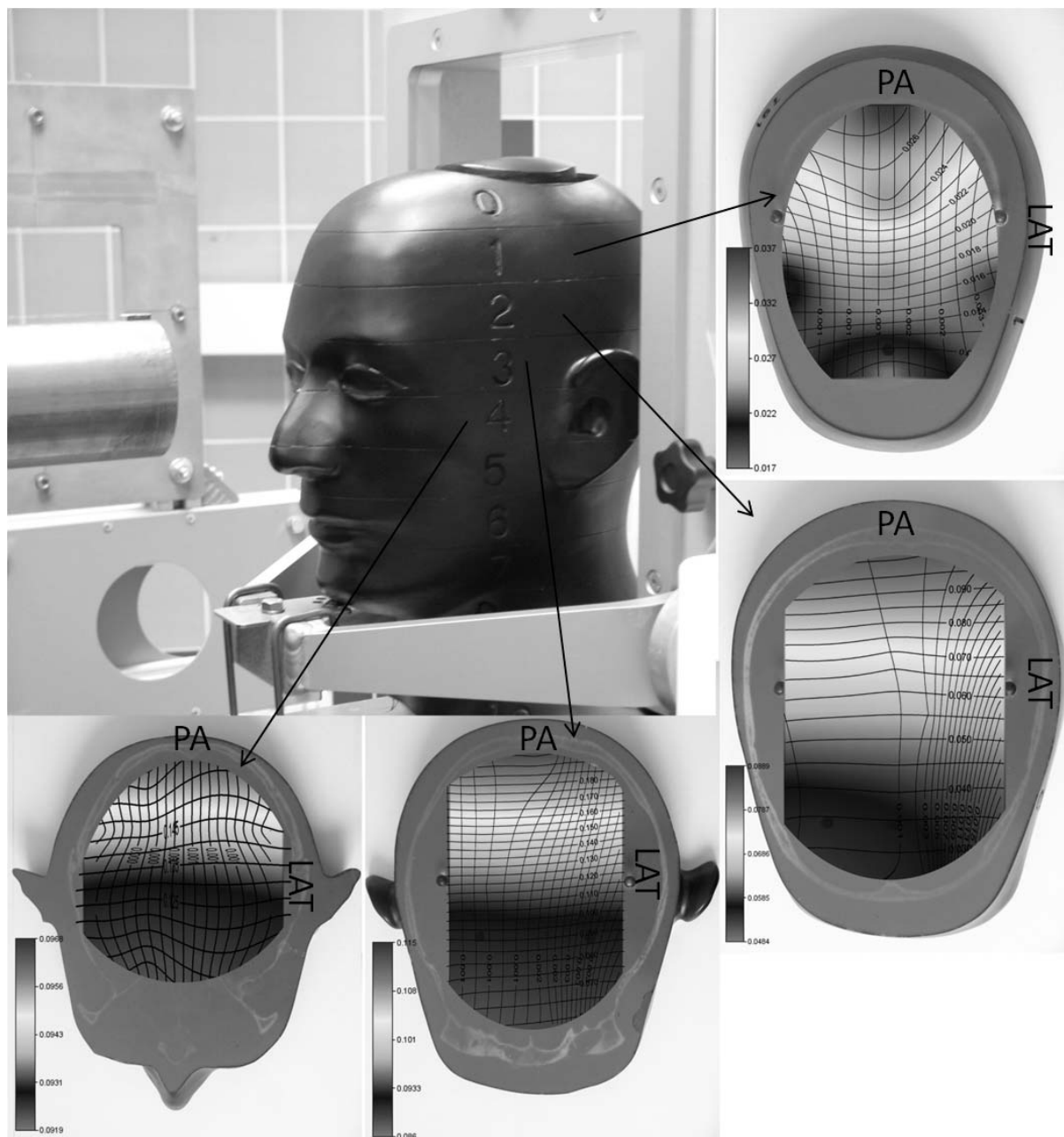


**Fig. 4.** Dose distribution in selected layers of the head of the Rando-Alderson phantom, obtained following five simultaneous exposures from both X-ray tubes (mGy). The colour scale ranges between 0.017 and 0.115 mGy.

## Conclusions

Results of several methods of measuring and calculating brain exposure due to the patient positioning procedure in proton ocular radiotherapy techniques have been compared. Whereas the dose estimations obtained with TLD's and small ionization chambers (0.3 and 30 cm<sup>3</sup>) were consistent, large volume (1000 cm<sup>3</sup>) ionization chamber can not be recommended because of the small radiation field. We assume that the total air kerma from X-ray exposures integrated over the whole positioning procedure will not exceed 15 or 7 mGy if filtration is added, and that the mean measured and calculated dose to the brain from this procedure is about 0.4 mGy. The additional patient dose due to patient positioning is negligible as compared to the dose levels used in radiotherapy.

Good agreement between the results of the measurements and those of PCXMC calculations indicates that our computer simulation represents the X-ray exposure setup to within some 20% or better. The PCXMC code applicable to the diagnostic radiology procedures can thus be very useful in determining the risk to the patient from multiple X-ray exposures during the positioning procedure required in the proton ocular radiotherapy. Whereas with a suitably represented measurement geometry, PCXMC calculations can provide a very good estimate of air kerma, the results of such calculations cannot be taken for granted and must always be verified by measurements with the use of appropriate dosimetry techniques.

**Acknowledgment.** Supported by a grant from Iceland, Liechtenstein and Norway through the EEA Financial Mechanism and the Norwegian Financial Mechanism.

## References

1. Decree of the Polish Cabinet (Minister of Health) concerning conditions of safe application of ionizing radiation for all types of medical exposures (2011) Dz U (Law Gazette) 18 February 2011, no 51, item 265 (in Polish)
2. Engel-Hills P (2006) Radiation protection in medical imaging. *Radiography* 12:153–160
3. Khelassi-Toutaouil N, Berkanil Y, Tsapaki V *et al.* (2008) Experimental evaluation of PCXMC and PREPARE codes used in conventional radiology. *Radiat Prot Dosim* 131;3:374–378
4. Martin CJ, Sutton DG, Sharp PF (1999) Balancing patient dose and image quality. *Appl Radiat Isot* 50:1–19
5. Olko P (2002) Microdosimetric modelling of physical and biological detectors. Habilitation Thesis. Report no. 1914/D. IFJ PAN, Kraków
6. PCXMC User's guide, Stuck – Radiation and Nuclear Safety Authority, Finland
7. Poludniowski G, Landry G, DeBlois F, Evans PM, Verhaegen F (2009) SpekCalc: a program to calculate photon spectra from tungsten anode X-ray tubes. *Phys Med Biol* 54:N433
8. PTW Freiburg Instruction Manual 1000 cm<sup>3</sup> Spherical Chamber Type TM32002
9. PTW Freiburg Instruction Manual 0.3 cm<sup>3</sup> Spherical Chamber Type 31013
10. PTW Freiburg Instruction Manual Ionization Chambers Type 31002 and Type 31003
11. RTI Electronics AB User Manual Ortigo QA Software for Barracuda and Piranha. Manual – English – Version 6.0A
12. Tapiovaara M, Siiskonen T (2008) PCXMC 2.0 User's Guide, STUK-TR 7
13. Wall BF (2004) Radiation protection dosimetry for diagnostic radiology patients. *Radiat Prot Dosim* 109;4:409–419
14. Wambersie A (2005) Patient dosimetry for X-rays used in medical imaging. *J ICRU* 5;2:I (doi:10.1093/jicru/ndi017)
15. Zoetelief J, Julius HW, Christen P (2003) Recommendations for patient dosimetry in diagnostic radiology using thermoluminescence dosimetry. International Commission on Radiation Units and IAEA activities. In: Proc of the Int Symp on Standards and Codes of Practice in Medical Radiation Dosimetry, 25–28 November 2002. IAEA-CN-96/49P. IAEA, Vienna, pp 439–447
16. Zoetelief J, Pernička F, Carlsson GA *et al.* (2003) Dosimetry in diagnostic and interventional radiology. International Commission on Radiation Units and IAEA activities. In: Proc of the Int Symp on Standards and Codes of Practice in Medical Radiation Dosimetry, 25–28 November 2002. IAEA-CN-96/39. IAEA, Vienna, pp 387–404